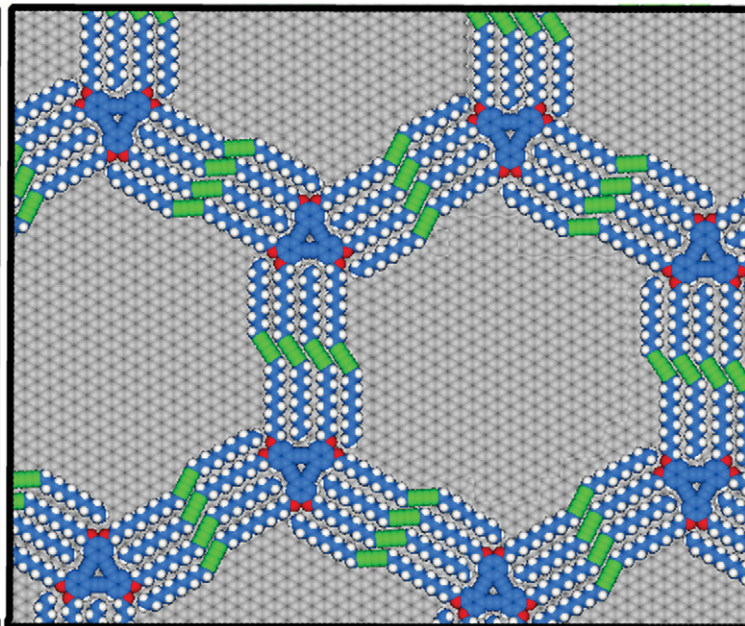
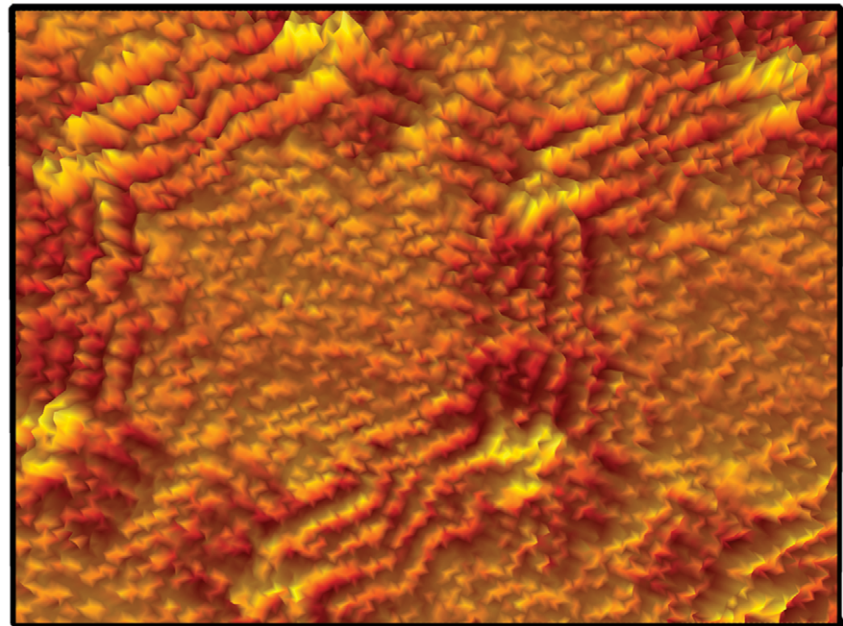
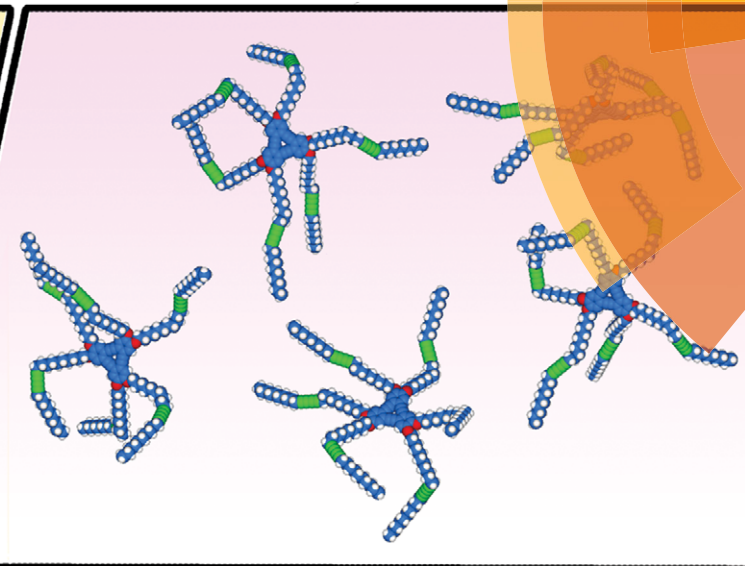
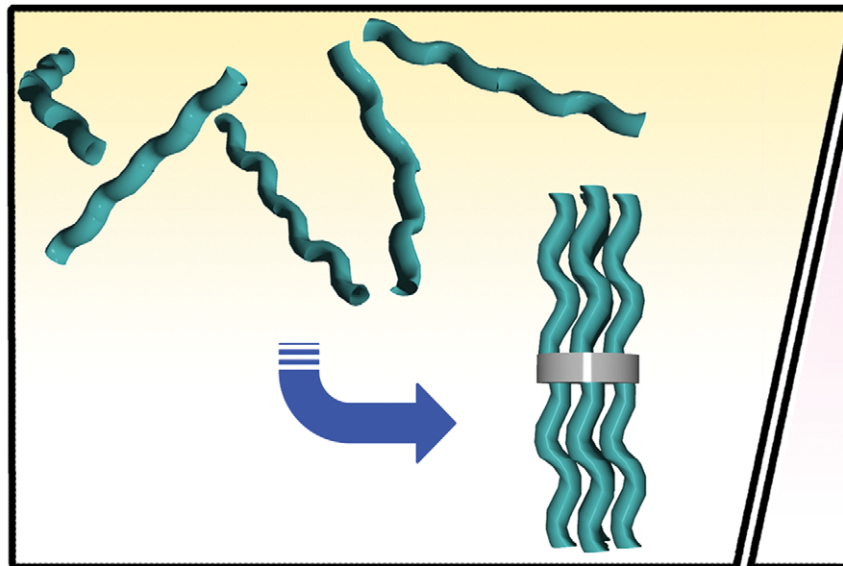


# ChemComm

Chemical Communications

[www.rsc.org/chemcomm](http://www.rsc.org/chemcomm)



ISSN 1359-7345



## COMMUNICATION

Steven De Feyter, Yoshito Tobe et al.

Harnessing by a diacetylene unit: a molecular design for porous two-dimensional network formation at the liquid/solid interface

# Harnessing by a diacetylene unit: a molecular design for porous two-dimensional network formation at the liquid/solid interface†

Kazukuni Tahara,<sup>‡,a</sup> Jinne Adisoejoso,<sup>‡,b</sup> Koji Inukai,<sup>a</sup> Shengbin Lei,<sup>b</sup> Aya Noguchi,<sup>a</sup> Bing Li,<sup>b</sup> Willem Vanderlinden,<sup>b</sup> Steven De Feyter<sup>\*b</sup> and Yoshito Tobe<sup>\*a</sup>

Cite this: *Chem. Commun.*, 2014, 50, 2831

Received 16th October 2013,  
Accepted 2nd December 2013

DOI: 10.1039/c3cc47949h

[www.rsc.org/chemcomm](http://www.rsc.org/chemcomm)

Through the precise molecular design for alkoxy dehydro[12]annulene derivatives harnessed by a diacetylene unit in each alkyl chain, porous two-dimensional networks with giant pores were formed at the liquid/graphite interface.

Surface confined two-dimensional (2D) molecular networks formed by self-assembly of organic molecules are a subject of interest from the perspective of various applications in the field of nanoscience and nanotechnology.<sup>1</sup> In particular, 2D porous molecular networks have received quite some attention due to the ability of these surface-confined molecular networks to accommodate guest molecules in the nanowells.<sup>2</sup> In general, the formation of porous molecular networks is thermodynamically unfavorable because of the low molecular surface density. Therefore, there are only few examples of 2D networks with pores or nanowells with diameters larger than 5 nm.<sup>3</sup> However, by a careful molecular design in combination with optimization of experimental conditions, such as solvent,<sup>4</sup> concentration<sup>5</sup> and temperature,<sup>6</sup> it should be possible to favor the formation of such large pores at the liquid/solid interface.

We have reported the formation of porous honeycomb-type structures of alkoxy dehydrobenzo[12]annulenes (DBAs, Fig. 1a) at the liquid/solid interface. The porous networks are stabilized by van der Waals interactions between interdigitated alkyl chains of adjacent molecules,<sup>7</sup> and the pore size can in principle be enlarged by elongation of the alkyl chain. However, nonporous structures were observed for the DBAs having relatively long alkoxy chains even at low solute concentrations.<sup>5c</sup> For instance, a DBA derivative with  $-OC_{30}H_{61}$  chains exhibited porous structures only in small areas even under submonolayer conditions.<sup>3a</sup> Therefore, it is a real

challenge to form stable 2D porous networks with large pore sizes, particularly at the liquid–solid interface.

Recently, Zimmt *et al.* reported that a kinked diacetylene (DA) unit in alkyl chains linked to anthracene cores could control 2D pattern formation *via* recognition of steric units that are complementary to the DA units.<sup>8</sup> We reasoned that the presence of a DA unit in the alkyl chains of DBAs would favor the formation and stabilization of 2D porous networks, even for large pore sizes, by reducing the toll on entropy that would otherwise be imposed for methylenes to adopt an all-*anti* conformation in the extended alkyl chains.<sup>9</sup> We planned to utilize this stabilizing effect of DA units to fabricate giant pores with a diameter of over 5 nm using DBA building blocks. We noted that a precise molecular design, more specifically the location of DA units, is a requisite to achieve optimal van der Waals interactions between alkyl chains. Moreover since four DA units would be aligned parallel in the interdigitated chains of porous networks of DBAs with DA units (DBA-DAs), these may serve as precursors of novel 2D polymers.<sup>10</sup>

Here we report the design and synthesis of **DBA-DA12.12**, **DBA-DA17.17**, **DBA-DA24.25** and **DBA-DA32.33** having DA units at different positions within the alkyl substituents (Fig. 1).

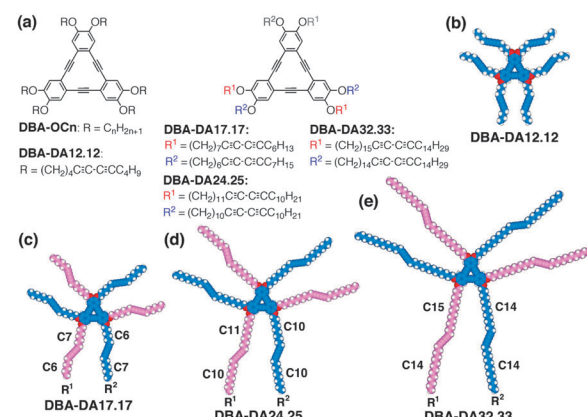


Fig. 1 (a) Chemical structures of **DBA-OCn** and **DBA-DAs**. (b)–(e) PM3 optimized molecular models of **DBA-DA12.12**, **DBA-DA17.17**, **DBA-DA24.25** and **DBA-DA32.33** under vacuum. In (c)–(e) different chains are colored in pink and blue.

<sup>a</sup> Division of Frontier Materials Science, Graduate School of Engineering Science, Osaka University, Toyonaka, Osaka 560-8531, Japan.

E-mail: [tobe@chem.es.osaka-u.ac.jp](mailto:tobe@chem.es.osaka-u.ac.jp); Tel: +81-(0)6-6850-6225

<sup>b</sup> Division of Molecular Imaging and Photonics, Department of Chemistry, KU Leuven, Celestijnenlaan 200 F, 3001 Leuven, Belgium.

E-mail: [steven.defeyter@chem.kuleuven.be](mailto:steven.defeyter@chem.kuleuven.be); Tel: +32-16-3-27921

† Electronic supplementary information (ESI) available: Experimental details, STM images, and syntheses of DBA-DAs. See DOI: 10.1039/c3cc47949h

‡ Both authors contributed equally to this work.

Self-assembly of the DBA-DAs was investigated at the 1,2,4-trichlorobenzene (TCB)/graphite interface using scanning tunnelling microscopy (STM). **DBA-DA24.25** and **DBA-DA32.33** formed honeycomb structures with giant pores having a diameter of 6 and 7 nm, respectively. Moreover, DBA-DAs formed the porous structures over wider concentration ranges compared to DBAs with saturated alkyl chains of comparable lengths, revealing the enhanced stabilization effect of the DA units on the porous network structures.

First we assume that the two alkoxy oxygen atoms attached to a benzene ring orient in a synclinal arrangement rather than in the same direction or in an anticlinal arrangement based on a theoretical study using the B3LYP/6-31g(d) level of theory (Fig. S1, ESI†). Hereafter we abbreviate the alkyl chains containing the DA unit as *m*-DA-*n* where *m* and *n* refer to the number of carbon atoms from the oxygen atom to the DA unit and from the DA unit to the terminal methyl group in the chain, respectively. Then we designed the simplest compound **DBA-DA12.12** having six identical chains (4-DA-4 chains). Molecular modeling of a dimer of **DBA-DA12.12** predicts that the four DA units cannot align parallel (Fig. S2a, ESI†). However, by changing the location of the DA unit in three of the alternating alkyl chains of **DBA-DA12.12** from 4-DA-4 to 3-DA-5, the modeling shows that all four DA units in the corresponding dimer can adopt parallel arrangement (Fig. S2b, ESI†). Based on these results, **DBA-DA17.17** comprising two different chains ( $R^1 = 6\text{-DA-7}$  and  $R^2 = 7\text{-DA-6}$ ; chain length is identical) in an alternating fashion was designed. The chains were elongated to increase intermolecular and molecule–substrate interactions and enlarge the pore size. Modeling predicts that **DBA-DA17.17** can form two structurally inequivalent honeycomb structures (type I and II) which differ in surface molecular density depending on the positions of  $R^1$  and  $R^2$  within the interdigitated four alkyl chains. To evaluate the relative stability of the type I and II structures, molecular mechanics simulations were performed using the hexamer models on a graphite lattice, in which the peripheral alkoxy chains were replaced by methoxy groups (Fig. 2, see ESI†). The possibility of solvent co-adsorption as a stabilizing effect was not taken into account in the simulations. As a result, the type II structure turned out to be more stable by  $10.7 \text{ kcal mol}^{-1}$  because of a non-ideal diacetylene

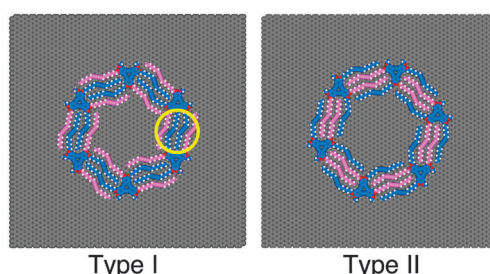


**Fig. 2** Optimized structures by the MM simulations (MM3 parameters) of the hexamer models formed by **DBA-DA17.17** with high (type I structure;  $a = b = 5.3 \text{ nm}$ ,  $\gamma = 60^\circ$  and  $d = 0.121 \text{ molecule nm}^{-2}$ ) and low (type II structure;  $a = b = 5.7 \text{ nm}$ ,  $\gamma = 60^\circ$  and  $d = 0.107 \text{ molecule nm}^{-2}$ ) molecular density. Side chains  $R^1$  (7-DA-6) and  $R^2$  (6-DA-7) are colored in blue and pink, respectively. In the type I structure, a gap and a shift between the inner DA units is indicated by a yellow circle.

packing and a small gap between the inner DA units in the type I structure.

To solve the mismatch in the type I structure of **DBA-DA17.17**, we designed **DBA-DA24.25** with alternating chains of different lengths, while keeping the length of the alkyl chain spacer between the DBA core and the diacetylene unit the same:  $R^1$  (10-DA-10) and  $R^2$  (10-DA-11) chains. In addition to the positive packing effects, the longer chain length should also lead to an enlarged pore size. The MM simulations for the type I and II structures of **DBA-DA24.25** predict no steric mismatch between the DA units in both cases (Fig. S3a, ESI†). The type I structure was more stable than the type II structure by  $12.7 \text{ kcal mol}^{-1}$ . In the latter structure, van der Waals contacts between the alkyl chains were smaller. Indeed, there is a small gap between the methyl groups at the end of alkyl chains and DBA cores.<sup>11</sup>

All these compounds were synthesized to test the predictions of modeling. In addition, **DBA-DA32.33** having two different long chains  $R^1$  (14-DA-14) and  $R^2$  (14-DA-15) was designed for the formation of even larger pores (Fig. S3b, ESI†). Syntheses of these four DBA-DAs are described in the ESI†.

A TCB solution of **DBA-DA12.12** ( $9.3 \times 10^{-4} \text{ M}$ ) was dropped on a graphite surface and examined by STM. However, monolayer formation was not observed, probably due to the significant structural mismatch of the DA units as predicted by modeling. In contrast, a structurally ordered monolayer of **DBA-DA17.17** was observed at the TCB/graphite interface. In the STM images (Fig. 3a and b), the bright features correspond to the conjugated cores of the DBA-DA molecules and the darker parts are composed of four interdigitated alkyl chains, revealing the formation of the honeycomb lattice. The observed domain size was larger than the typical scanning size ( $10000 \text{ nm}^2$ ). Surprisingly, comparison of the structural parameters with those calculated by the MM simulations (Fig. 2, Table S1, ESI†) revealed the formation of the type I honeycomb structure. This observation is in contrast with the relative stability predicted by the MM simulations indicating that in this case the network structure is controlled by the molecular surface density rather than the intermolecular interactions. Another possibility is a stabilization effect by co-adsorption of solvent molecules in the pore.

In **DBA-DA24.25**, large domains of the honeycomb structure were observed at the TCB/graphite interface (Fig. 4a and b). “Kinks” due to the DA units are clearly observed in the middle of the alkyl chains.<sup>12</sup> Comparison of the unit cell parameters with those predicted by the MM simulations (Fig. S3a and

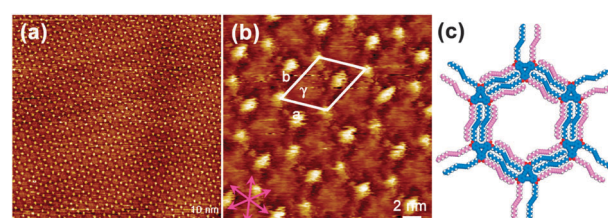


**Fig. 3** STM images (a, b) and a molecular model (c) of the monolayer formed by **DBA-DA17.17** at the TCB/graphite interface. Tunneling parameters are  $I_{\text{set}} = 0.21 \text{ nA}$ ,  $V_{\text{set}} = -0.84 \text{ V}$  for (a) and  $I_{\text{set}} = 0.17 \text{ nA}$ ,  $V_{\text{set}} = -0.79 \text{ V}$  for (b), respectively. Unit cell parameters are  $a = b = 5.3 \pm 0.1 \text{ nm}$  and  $\gamma = 61 \pm 3^\circ$ . The concentration of **DBA-DA17.17** is  $8.2 \times 10^{-4} \text{ M}$ .

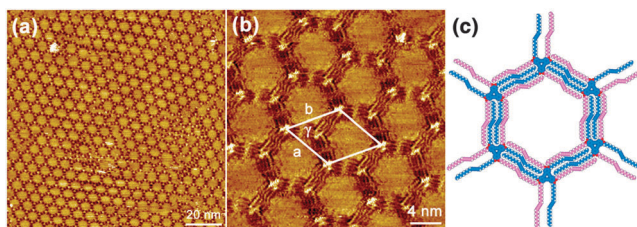


**Fig. 4** STM images (a, b) and a molecular model (c) of the monolayer formed by **DBA-DA24.25** at the TCB/graphite interface. Tunneling parameters are  $I_{\text{set}} = 0.1 \text{ nA}$ ,  $V_{\text{set}} = -1.0 \text{ V}$  for (a) and  $I_{\text{set}} = 0.1 \text{ nA}$ ,  $V_{\text{set}} = -1.0 \text{ V}$  for (b), respectively. Unit cell parameters are  $a = b = 7.0 \pm 0.1 \text{ nm}$ , and  $\gamma = 60 \pm 2^\circ$ . The concentration of **DBA-DA24.25** is  $1.9 \times 10^{-6} \text{ M}$ .

**Table S1, ESI†**) confirmed the formation of the more dense type I honeycomb structure. The pore diameter reaches 6.0 nm (the distance across the DA units). Also **DBA-DA32.33** formed a porous monolayer network at the TCB/graphite interface (Fig. 5). DA units are clearly observed as bright lines in the middle of interdigitated alkyl chains. The diameter of the pore becomes *ca.* 7 nm (distance between the DA units). The typical domain size is smaller than the other DBA-DAs though, and the degree of order is lower. However, in contrast to the monolayer of **DBA-OC30**, so lacking DA units,<sup>3a</sup> nonporous densely packed structures were scarcely observed at low concentrations.

The honeycomb structures formed by DBA-DAs at the TCB/graphite interface were observed over a wide concentration range reflecting the stabilization effect of the DA units. Similar to DBAs,<sup>5c</sup> DBA-DAs were shown to exhibit polymorphism between the porous and nonporous structures depending on the solute concentration. In order to qualitatively compare the increased stability provided by the DA units, the observed proportion of porous networks was probed as a function of solute concentration and compared to **DBA-OC18**.<sup>5c</sup> **DBA-OC18** only formed porous structures at a concentration lower than  $1.0 \times 10^{-6} \text{ M}$  (Fig. S6, ESI†). In contrast, porous structures are formed at a concentration lower than  $1.9 \times 10^{-6} \text{ M}$  for **DBA-DA24.25** and  $9.2 \times 10^{-7} \text{ M}$  for **DBA-DA32.33**, despite the lower molecular surface densities of the porous networks of the DBA-DAs ( $0.07$  and  $0.05$  molecule  $\text{nm}^{-2}$ ) with respect to **DBA-OC18** ( $0.10$  molecule  $\text{nm}^{-2}$ ). In general, given the lower molecular surface densities and larger pore sizes, at the same concentration, the proportion of porous networks is always larger for DBA derivatives with DA units in their chains. These results indicate that by incorporating DA units within the rims of the pores, porous

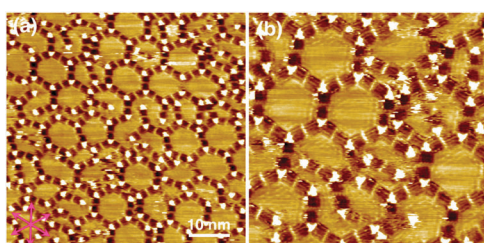


**Fig. 5** STM images (a, b) of the monolayer formed by **DBA-DA32.33** at the TCB/graphite interface. Tunneling parameters are  $I_{\text{set}} = 0.1 \text{ nA}$ ,  $V_{\text{set}} = -0.70 \text{ V}$  for (a) and  $I_{\text{set}} = 0.1 \text{ nA}$ ,  $V_{\text{set}} = -0.70 \text{ V}$  for (b), respectively. The concentration of **DBA-DA32.33** is  $9.2 \times 10^{-7} \text{ M}$ .

networks can be further stabilized. Moreover, the porous network of **DBA-DA24.25** was found to be stable enough to preserve its structure after solvent evaporation (Fig. S7, ESI†).<sup>8</sup>

We have shown that through a precise design of DBA derivatives having a diacetylene unit in each alkyl chain porous networks with giant 2D pores can be stabilized at the liquid/solid interface. The diameters of the pores reached 6 and 7 nm for **DBA-DA24.25** and **DBA-DA32.33**, respectively. Upon simply introducing diacetylene units within the alkyl chains, the resultant porous hexagonal networks were observed to be more stable than their counterparts that lack the diacetylene units. The present knowledge is important for the construction of porous networks with giant pores and for 2D crystal engineering in general. Investigation on interlinking the DA units aiming at porous 2D polymer synthesis is currently underway.

This work was supported by the Grant-in-Aid for Scientific Research from the Ministry of Education, Culture, Sports, Science, and Technology, Japan (19750033, 21245012, 23111710), the Fund of Scientific Research – Flanders (FWO), KU Leuven (GOA), and the Belgian Federal Science Policy Office through IAP-7/05. The research leading to these results has also received funding from the European Research Council under the European Union's Seventh Framework Programme (FP7/2007–2013)/ERC Grant Agreement no. 340324.

## Notes and references

- (a) J. V. Barth, *Annu. Rev. Phys. Chem.*, 2007, **58**, 375–407; (b) J. V. Barth, G. Costantini and K. Kern, *Nature*, 2005, **437**, 671–679; (c) J. A. A. W. Elemans, L. S. Lei and S. De Feyter, *Angew. Chem., Int. Ed.*, 2009, **48**, 7298–7332.
- (a) D. Bonifazi, S. Mohnani and A. Llanes-Pallas, *Chem.–Eur. J.*, 2009, **15**, 7004–7025; (b) X. Ma, Y. Yang, K. Deng, Q. Zeng, K. Zhao, C. Wang and C. Bai, *J. Mater. Chem.*, 2008, **18**, 2074–2081.
- (a) K. Tahara, S. Lei, D. Mössinger, H. Kozuma, K. Inukai, M. Van der Auweraer, F. C. De Schryver, S. Höger, Y. Tobe and S. De Feyter, *Chem. Commun.*, 2008, 3897–3899; (b) D. Kühne, F. Klappenberg, R. Decker, U. Schlickum, H. Brune, S. Klyatskaya, M. Ruben and J. V. Barth, *J. Am. Chem. Soc.*, 2009, **131**, 3881–3883.
- Y. Yang and C. Wang, *Curr. Opin. Colloid Interface Sci.*, 2009, **14**, 135–147.
- (a) L. Kampschulte, T. L. Werblowsky, R. S. K. Kishore, M. Schmittel, W. M. Heckl and M. Lackinger, *J. Am. Chem. Soc.*, 2008, **130**, 8502–8507; (b) C.-A. Palma, J. Bjork, M. Bonini, M. S. Dyer, A. Llanes-Pallas, D. Bonifazi, M. Persson and P. Samori, *J. Am. Chem. Soc.*, 2009, **131**, 13062–13071; (c) S. Lei, K. Tahara, F. C. De Schryver, M. Van der Auweraer, Y. Tobe and S. De Feyter, *Angew. Chem., Int. Ed.*, 2008, **47**, 2964–2968.
- (a) R. Gutzler, T. Sirtl, J. F. Dienstmaier, K. Mahata, W. M. Heckl, M. Schmittel and M. Lackinger, *J. Am. Chem. Soc.*, 2010, **132**, 5084–5090; (b) A. Bellec, C. Arrigoni, G. Schull, L. Douillard, C. Fiorini-Debuisschert, F. Mathevet, D. Kreher, A.-J. Attias and F. Charra, *J. Chem. Phys.*, 2011, **134**, 124702; (c) M. O. Blunt, J. Adisojoso, K. Tahara, K. Katayama, M. Van der Auweraer, Y. Tobe and S. De Feyter, *J. Am. Chem. Soc.*, 2013, **135**, 12068–12075.
- (a) K. Tahara, S. Furukawa, H. Uji-i, T. Uchino, T. Ichikawa, J. Zhang, W. Mamdouh, M. Sonoda, F. C. De Schryver, S. De Feyter and Y. Tobe, *J. Am. Chem. Soc.*, 2006, **128**, 16613–16625; (b) K. Tahara, S. Lei, J. Adisojoso, S. De Feyter and Y. Tobe, *Chem. Commun.*, 2010, **46**, 8507–8525.
- Y. Xue and M. B. Zimmt, *Chem. Commun.*, 2011, **47**, 8832–8834.
- E. L. Eliel and S. H. Wilen, *Stereochemistry of organic compounds*, Jhon Wiley & Sons, New York, 1994, pp. 601–604.
- (a) J. Sakamoto, J. van Heijst, O. Lukin and A. D. Schlüter, *Angew. Chem., Int. Ed.*, 2009, **48**, 1030–1069; (b) J. W. Colson and W. R. Dichtel, *Nat. Chem.*, 2013, **5**, 453–465.
- E. Ghijssens, O. Ivasenko, K. Tahara, H. Yamaga, S. Itano, T. Balandina, Y. Tobe and S. De Feyter, *ACS Nano*, 2013, **7**, 8031–8042.
- In other solvents such as 1-phenyloctane, tetradecane, and 1-octanoic acid, **DBA-DA24.25** formed non-porous structures. Such solvent effect was reported previously. See ref. 7.